Clays and Clay Minerals, Vol. 60, No. 6, 588–598, 2012.

AN ELECTRON PARAMAGNETIC RESONANCE SPECTROSCOPY INVESTIGATION OF THE RETENTION MECHANISMS OF Mn AND Cu IN THE NANOPORE CHANNELS OF THREE ZEOLITE MINERALS

DANIEL R. FERREIRA[1,*], CRISTIAN P. SCHULTHESS[2], JAMES E. AMONETTE[3], AND ERIC D. WALTER[3]

[1] Department of Biology and Chemistry, Southern Polytechnic State University, Building E, Suite 183, 1100 South Marietta Pkwy, Marietta, GA 30060, USA

[2] Department of Plant Science and Landscape Architecture, University of Connecticut, 1376 Storrs Road, Storrs, CT 06269-4067, USA

[3] Pacific Northwest National Laboratory, 902 Battelle Boulevard, P.O. Box 999 Richland, WA 99352, USA

Abstract—The adsorption mechanisms of divalent cations in zeolite nanopore channels can vary as a function of their pore dimensions. The nanopore inner-sphere enhancement (NISE) theory predicts that ions may dehydrate inside small nanopore channels in order to adsorb more closely to the mineral surface if the nanopore channel is sufficiently small. The results of an electron paramagnetic resonance (EPR) spectroscopy study of Mn and Cu adsorption on the zeolite minerals zeolite Y (large nanopores), ZSM-5 (intermediate nanopores), and mordenite (small nanopores) are presented. The Cu and Mn cations both adsorbed *via* an outer-sphere mechanism on zeolite Y based on the similarity between the adsorbed spectra and the aqueous spectra. Conversely, Mn and Cu adsorbed *via* an inner-sphere mechanism on mordenite based on spectrum asymmetry and peak broadening of the adsorbed spectra. However, Mn adsorbed *via* an outer-sphere mechanism on ZSM-5, whereas Cu adsorbed on ZSM-5 shows a high degree of surface interaction that indicates that it is adsorbed closer to the mineral surface. Evidence of dehydration and immobility was more readily evident in the spectrum of mordenite than in that of ZSM-5, indicating that Cu was not as close to the surface on ZSM-5 as it was when adsorbed on mordenite. Divalent Mn cations are strongly hydrated and are held strongly only in zeolites with small nanopore channels. Divalent Cu cations are also strongly hydrated, but can dehydrate more easily, presumably due to the Jahn-Teller effect, and are held strongly in zeolites with medium-sized nanopore channels or smaller.

Key Words—Adsorption, Copper, EPR, Inner-sphere, Ion Exchange, Manganese, Nanopores, NISE, Outer-sphere, Zeolites.

INTRODUCTION

The retention of ions by mineral surfaces plays a vital role in many critical environmental processes such as nutrient availability and contaminant mobility. Many factors regulate how ions move between the solid and aqueous environments. Understanding how these factors function and interrelate is critical if we wish to understand ion exchange processes occurring in the natural environment. The factors involved include the nature of the adsorbate (such as its charge), the nature of the adsorbent (such as its chemical composition), and the adsorption mechanism of the adsorbing ion. An ion can bond directly to the surface of a mineral (inner-sphere bonding), or it can bond to a mineral through one or more layers of water molecules (outer-sphere bonding). Ions which adsorb *via* an inner-sphere mechanism are generally more strongly retained than ions which adsorb *via* an outer-sphere mechanism (Sposito, 1989). Recent studies have shown that the physical dimensions of the adsorbent are also important. For example, adsorption envelopes for Na, K, and Ca on the zeolite mineral ZSM-5 (Table 1) showed that both Na and K adsorbed strongly, while Ca adsorbed weakly (Ferreira and Schulthess, 2011). Under most conditions, it is unusual for a monovalent ion to outcompete a divalent ion at equimolar concentrations for adsorption sites. Additional studies on ZSM-5 showed a very weak impact by Mg or Ba ions on the strong adsorption of Na ions at equimolar concentrations (Ferreira, 2012).

In order to explain this unusual adsorption selectivity, Schulthess *et al.* (2011) proposed the NISE theory based on adsorption data for Ni and Na on three different zeolites. The NISE theory states that the ability of an ion to adsorb on an adsorption site located inside a nanopore channel will increase significantly if the ion's ability to dehydrate is enhanced by the physical environment of the adsorption site. Predicting the ion's propensity to dehydrate is based primarily on its hydration energy, but other properties that influence the hydration sphere may be involved. When a cation is attracted to an adsorption site inside a nanopore channel that is smaller than its hydrated diameter, the cation may dehydrate in order to enter the nanopore and adsorb. Under such conditions, the more weakly hydrated a cation is, the more easily it will

* E-mail address of corresponding author:
DFerreira@spsu.edu
DOI: 10.1346/CCMN.2012.0600604

Table 1. Zeolite characteristics: zeolite codes and pore dimensions from the database of zeolite structures (www.iza-structure.org).

Zeolite name	Zeolite code	– Dimensions (nm) – Pore 1	Pore 2	SiO_2:Al_2O_3 ratio
Zeolite Y	FAU	0.74 × 0.74	n/a	80:1
ZSM-5	MFI	0.51 × 0.55	0.53 × 0.56	80:1
Mordenite	MOR	0.70 × 0.65	0.26 × 0.57	90:1

dehydrate and adsorb *via* a stronger inner-sphere mechanism. As divalent ions are more strongly hydrated than monovalent ions of similar size (Collins, 1997), this puts divalent ions at a distinct disadvantage when competing against monovalent ions inside small nanopore channels. Accordingly, monovalent ions show greater adsorption in the nanopore channels of zeolites like ZSM-5 because the confining environment stabilizes them as dehydrated inner-sphere complexes. The divalent cations, on the other hand, have a large hydration energy. As a result, they retain some of their hydrating water molecules and adsorb *via* a weaker outer-sphere mechanism.

A calorimetry study of ion-exchange processes on the zeolite minerals zeolite Y, ZSM-5, and mordenite was conducted recently. The results showed that Na ions were able to easily outcompete Ca ions in the intermediate nanopore channels of the zeolite mineral ZSM-5 at equal charge densities (Ferreira *et al.*, 2013). The data showed that the removal of Ca from the exchange complex by Na adsorption on this zeolite was fast and highly energetic. The attempt to remove Na from the exchange complex by Ca, on the other hand, was a slow and gradual process that showed limited success. This supports the predictions made by the NISE theory that Na adsorbs *via* an inner-sphere mechanism on ZSM-5 while Ca adsorbs *via* an outer-sphere mechanism.

Nuclear magnetic resonance (NMR) spectroscopy has also confirmed the predictions made by the nanopore inner-sphere enhancement (NISE) theory concerning the adsorption of Na ions inside the nanopore channels of the same three zeolite minerals (Ferreira *et al.*, 2012). Specifically, Na adsorbed *via* an outer-sphere mechanism in the large nanopores of zeolite Y, but *via* an inner-sphere mechanism in the smaller nanopores of ZSM-5 and mordenite. That NMR study did not include divalent ions because the detection limits of NMR instruments are highly dependent on the precession frequency of the atom being studied. Non-magnetic divalent ions have a low precession frequency, which makes them difficult to analyze using nuclear magnetic resonance (NMR) spectroscopy. As the NISE theory makes predictions for the adsorption behavior of both monovalent and divalent ions, spectroscopic evidence of the adsorption mechanisms of divalent ions on the same zeolite minerals would more fully validate the NISE theory.

Electron paramagnetic resonance (EPR) spectroscopy is capable of detecting many divalent ions with a high degree of precision. In particular, Mn and Cu are both suitable for EPR spectroscopy and many studies of the EPR spectra of these ions under varying conditions are in the literature (Turkevich *et al.*, 1972; Hronský *et al.*, 1978; Larsen *et al.*, 1994; Bergaoui *et al.*, 1995; Carl and Larsen, 2000). In order to further validate the NISE theory for divalent ions, the results of an EPR study of Mn and Cu on zeolite Y, ZSM-5, and mordenite are presented here. Both ions have a strong total hydration energy, but Cu is subject to the Jahn-Teller effect, which influences the coordination of its hydration sphere.

Calcium and the other alkaline earth divalent cations discussed above do not have unpaired electrons and are, therefore, not suitable for EPR analysis. Instead, Mn and Cu were used in this study to elucidate the adsorption mechanisms of divalent ions on three zeolites. Adsorption envelopes for Mn and Cu on the same three zeolites were collected so that the relative magnitude of retention could also be interpreted in terms of the NISE theory. Once the adsorption of Mn and Cu was measured, EPR studies were conducted to verify the predictions made by the NISE theory concerning their adsorption mechanisms as a function of the zeolite pore sizes.

MATERIALS AND METHODS

Zeolite minerals

The zeolites used in this study were purchased from Zeolyst International (Conshohocken, Pennsylvania, USA). Mordenite and zeolite Y were purchased as hydrogen forms, meaning that their surfaces had only hydrogen ions adsorbed. ZSM-5 was purchased as an ammonium form, and was converted to a hydrogen form through the volatilization of NH_4^+ to NH_3 gas, leaving only H^+ ions behind. This process was described in greater detail by Schulthess *et al.* (2011). The three zeolites are essentially chemically identical with similar SiO_2:Al_2O_3 ratios of 80:1 for zeolite Y and ZSM-5 and 90:1 for mordenite (Table 1). The zeolites differ primarily in the dimensions of their nanopore channels. The dissolution of these zeolites was shown to be negligible down to pH 1 (Ferreira and Schulthess, 2011).

EPR analysis

Samples for EPR analysis were prepared by adding 0.500±0.005 g of zeolite Y, ZSM-5, or mordenite to a

https://doi.org/10.1346/CCMN.2012.0600604 Published online by Cambridge University Press

centrifuge tube, along with doubly deionized water, 0.12 M HNO_3, 0.1 M $Mn(NO_3)_2$ or 0.1 M $Cu(NO_3)_2$, and 0.1 M NaOH. Each sample had 7 mL of NaOH added to it. The pH was adjusted downward using varying amounts of HNO_3. The pH was adjusted in this way to maintain a constant Na concentration of 20 mM in all samples. This same concentration of $Mn(NO_3)_2$ or $Cu(NO_3)_2$ was also used to allow for equimolar competition between Na and the divalent cations. Each centrifuge tube had a total liquid volume of 35 mL.

The samples for EPR analysis were shaken on an orbital mixer for 18–20 h and allowed to equilibrate. They were then centrifuged at 8700 × g for 10 min using a Beckman GS-15 centrifuge to separate the solid and liquid phases. The bulk of the liquid was then decanted, and the remaining solid and liquid were separated by filtration using a Lida Manufacturing 0.45 μm pore-size centrifuge filter in a Labnet Z100A centrifuge at 1900 × g for 25 min. The solid phase was then washed with deionized water to remove any aqueous ions so that only adsorbed ions would be detected. The solid and the supernatant for each sample were then pulled into capillary tubes for EPR analysis using a syringe.

The EPR analyses were conducted at room temperature (~20ºC) using a Bruker 380E 9.5 GHz X-band electron paramagnetic resonance spectrometer with a Bruker ER4102ST (TE_{102} mode) standard cavity probe. Instrument operating parameters are presented in Table 2.

Adsorption envelopes

The samples used to generate adsorption envelopes had zeolite solid, doubly deionized water, HNO_3, NaOH, and $Mn(NO_3)_2$ or $Cu(NO_3)_2$ added to centrifuge tubes as described above. They were equilibrated on a hematology mixer for 18–20 h and then centrifuged at 7800 × g for 10 min. An aliquot of the supernatant liquid was then extracted and analyzed for pH as well as Na and Mn or Cu concentration. Aqueous ion concentrations were analyzed with High Performance Liquid Chromatography (HPLC) using a Hamilton PRP-X800 7 μm column with a flow rate of 1 mL min^{-1} of 4 mM HNO_3 and a Shimadzu CDD-10A conductivity detector. Some samples had aqueous ion concentrations measured using inductively coupled plasma-optical emission spectroscopy (ICP-OES, Spectro CROS Vision Argon Plasma Spectrometer, Spectro Analytical, Mahwah, New Jersey, USA) to verify the accuracy of the HPLC analysis.

Adsorbed ion distance calculations

Part 1. Estimation of number of unit cells present in each sample. The unit cell formula for the dry H-form of zeolite Y is $H_n[Al_nSi_{192-n}O_{384}]$. This zeolite had a SiO_2/Al_2O_3 molar ratio of 80:1, which resulted in n = 4.68, where $40 \cdot n = 192 - n$. The formula weight was 11,535.68 g mol^{-1}. A 0.5 g sample, therefore, had 43.34 μmol of unit cells present.

The unit-cell formula for the dry H-form of ZSM-5 is $H_n[Al_nSi_{96-n}O_{192}]$. This zeolite had a SiO_2/Al_2O_3 molar ratio of 80:1, which resulted in n = 2.34, where $40 \cdot n = 96 - n$. The formula weight was 5767.839 g mol^{-1}. A 0.5 g sample thus had 86.688 μmol of unit cells present.

The unit cell formula for the dry H-form of mordenite is $H_n[Al_nSi_{48-n}O_{96}]$. This zeolite had a SiO_2/Al_2O_3 molar ratio of 90:1, which resulted in n = 1.04, where $45 \cdot n = 48 - n$. The formula weight was 2883.93 g mol^{-1}. A 0.5 g sample thus had 173.37 μmol of unit cells present.

Part 2: Estimation of total μmol of adsorbed metal cation on each zeolite. The amount of metal adsorbed is shown in the adsorption envelopes (Figures 1 and 2). At pH 2.5, Cu adsorption was 0.1250 μmol m^{-2} on 0.5 g of zeolite Y with surface area of 700 m^2 g^{-1}. This resulted in 43.75 μmol Cu adsorbed per sample, equivalent to (0.125 μmol m^{-2})·(0.5 g $sample^{-1}$)·(700 m^2 g^{-1}). Similarly, at pH 5.3, Mn adsorption on zeolite Y was 0.0551 μmol m^{-2}, which resulted in 19.285 μmol Mn adsorbed per sample.

Adsorption of Cu at pH 2.5 was 0.2676 μmol m^{-2} on 0.5 g of ZSM-5 with surface area of 425 m^2 g^{-1}. This resulted in 56.86 μmol Cu adsorbed per sample, equivalent to (0.2676 μmol m^{-2})·(0.5 g $sample^{-1}$)·(425 m^2 g^{-1}). Similarly, at pH 5.3, Mn adsorption on

Table 2. EPR instrument operating parameters.

Sample ID	Scan range (G)	Scan density (points G^{-1})	Attenuation (db)	Power (μW)	Frequency (GHz)
Mn, aqueous	3,084–3,884	1.28	50	1.98	9.760427
Mn, zeolite Y	1,284–4,400	1.31	10	19.73	9.855598
Mn, ZSM-5	1,284–4,400	1.31	10	19.73	9.856472
Mn, mordenite	1,284–4,400	1.31	10	19.73	9.855822
Cu, aqueous	1,550–2,500	2.17	30	0.19	9.854956
Cu, zeolite Y	1,550–2,500	2.17	10	19.73	9.855912
Cu, ZSM-5	1,550–2,500	2.17	10	19.73	9.856225
Cu, mordenite	1,550–2,500	2.17	10	19.73	9.855694

https://doi.org/10.1346/CCMN.2012.0600604 Published online by Cambridge University Press

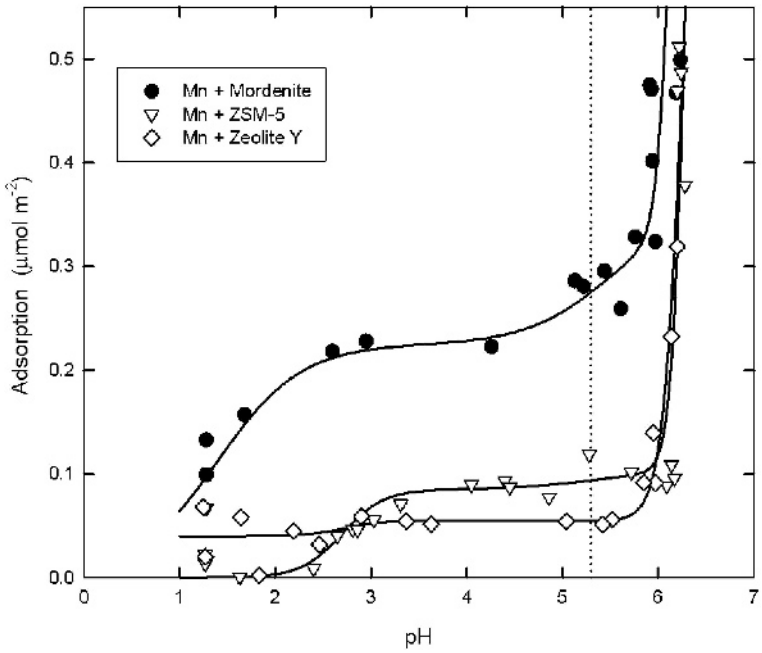

Figure 1. Adsorption envelopes of Mn on zeolite Y (large nanopores), ZSM-5 (medium nanopores), and mordenite (large and small nanopores). The dotted line indicates the pH during the EPR scans.

ZSM-5 was 0.0939 μmol m^{-2}, which resulted in 19.95 μmol Mn adsorbed per sample.

Adsorption of Cu at pH 2.5 was 0.3460 μmol m^{-2} on 0.5 g of mordenite with surface area of 500 m^2 g^{-1}. This resulted in 86.50 μmol Cu adsorbed per sample, equivalent to (0.3460 μmol m^{-2})·(0.5 g $sample^{-1}$)·(500 m^2 g^{-1}). Similarly, at pH 5.3, Mn adsorption on mordenite was 0.2753 μmol m^{-2}, which resulted in 68.825 μmol Mn adsorbed per sample.

Part 3: Estimation of the number of unit cells occupied by each adsorbed ion. Dividing the number of unit cells

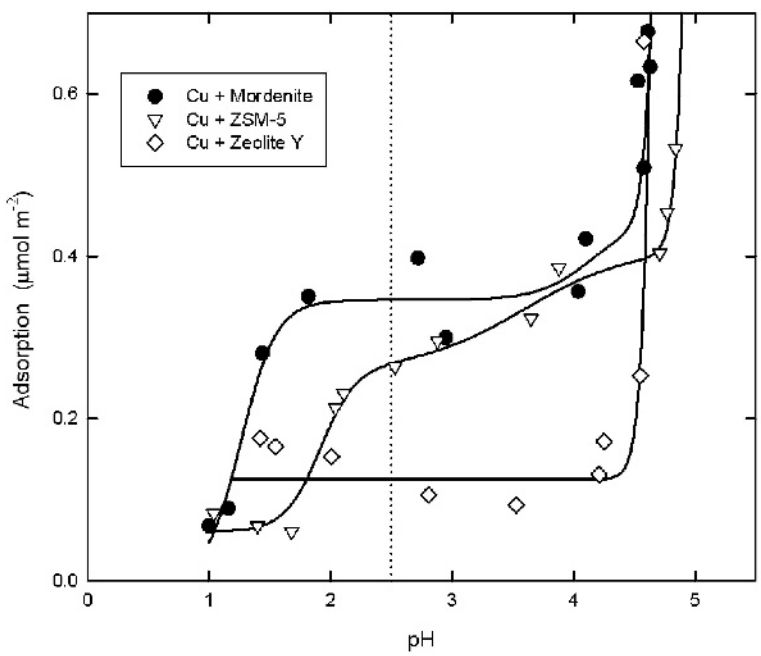

Figure 2. Adsorption envelopes of Cu on zeolite Y (large nanopores), ZSM-5 (medium nanopores), and mordenite (large and small nanopores). The dotted line indicates the pH during the EPR scans.

https://doi.org/10.1346/CCMN.2012.0600604 Published online by Cambridge University Press

present in the sample by the number of ions adsorbed by the sample yields the average number of cells for each adsorbed ion. Accordingly, for Cu: 43.34/43.75 = 0.99 for zeolite Y, 86.688/56.86 = 1.52 for ZSM-5, and 173.37/86.50 = 2.00 for mordenite. Similarly, for Mn: 43.34/19.285 = 2.25 for zeolite Y, 86.688/19.95 = 4.35 for ZSM-5, and 173.37/68.825 = 2.52 for mordenite.

Part 4: Estimation of the mean distance between ions adsorbed to zeolite Y. The zeolite Y structure consists of interconnected pore channels with no clearly defined adsorption sites. The adsorption sites in these channels should reside as far apart from each other as possible if an homogenous solid solution is assumed for the adsorption sites. As each unit cell contains one Cu ion, the estimated distance between each of these ions was one unit in any direction. The cell dimensions are: $a = b = c = 2.4345$ nm. Accordingly, the Cu−Cu distances are ~2.4 nm.

Each Mn ion occupied 2.25 unit cells. As each unit cell occupied 14.429 nm^3, each Mn ion occupied 32.465 nm^3. The cube root yields the average Mn−Mn distance as ~3.2 nm.

Part 5: Estimation of the mean distance between ions adsorbed to ZSM-5. The unit-cell dimensions of ZSM-5 are: $a = 2.01$ nm, $b = 2.00$ nm, and $c = 1.34$ nm. Once again, as the pore channels have no clearly defined adsorption sites, one can assume that an homogenous solid solution is present for the adsorption sites. Each Cu ion occupies 1.52 unit cells, which resulted in Cu−Cu distances of ~2.0 nm. The separation in the c direction is $1.52\ c = 2.0$ nm, and the separation in the a and b directions equals the unit-cell dimensions.

Each Mn ion occupies 4.35 unit cells. This is a large volume, which allows one to estimate the ion distances based on the cube root of the volume occupied, where the volume occupied by each ion is $4.35(a{\cdot}b{\cdot}c) = 23.43$ nm^3. Accordingly, the cube root yields 2.86 nm for the approximate average distance of the Mn−Mn separation.

Part 6: Estimation of the mean distance between ions adsorbed to mordenite. The unit-cell dimensions of mordenite are: $a = 1.81$ nm, $b = 2.05$ nm, and $c = 0.75$ nm. Alberti *et al.* (1986) showed that the Al sites are located primarily in the tetrahedra of the 4-member rings on the edges of the 8-member ring channels. Simoncic and Armbruster (2004) showed that the non-framework cations are found inside the 8-member rings. The SiO_2:Al_2O_3 ratio of the mordenite used in this study was very high, which resulted in a high value of 2.00 unit cells per adsorbed Cu ion. Placing these two cells over each other in the c direction and with an alternating placement of the Cu ions between the a and b edges results in a Cu−Cu separation of 3.0 nm ($= 4{\cdot}c$) in the c direction. The Cu−Cu distance from those in the alternating edges is 2.03 nm ($= [(a/2)^2 + (b/2)^2 + (2c)^2]^{0.5}$). Within the same ab plane, the Cu−Cu separation distances are 1.81 and 2.05 nm.

Each Mn ion occupied 2.52 unit cells, which is equivalent to two Mn ions for every five unit cells. These Mn ions can be arranged so that they are below each other in every third cell, or $3{\cdot}c = 2.25$ nm. The nearest Mn−Mn distance is 1.96 nm ($= (b^2 + c^2)^{0.5}$), which occurs between adjacent cells in the b direction offset by one c distance. All other Mn−Mn distances range from 2.18 nm to 6.15 nm.

RESULTS AND DISCUSSION

Adsorption

Adsorption experiments for the Mn ion on three zeolite minerals complement the adsorption selectivity patterns established by Ferreira and Schulthess (2011) for Na, K, and Ca on the same zeolites. Adsorption envelopes for Mn on the three zeolite minerals showed weak adsorption on zeolite Y (large nanopores) and ZSM-5 (medium nanopores), and strong adsorption on mordenite (small nanopores) (Figure 1). These results are similar to the selectivity patterns observed by Ferreira and Schulthess (2011) for Ca adsorption on these same zeolites at the same initial concentration. They contrast, however, with the results obtained for the monovalent cations Na and K, which adsorbed strongly at the same initial concentration in the medium nanopores of ZSM-5.

Adsorption envelopes for Cu showed weak adsorption on zeolite Y and strong adsorption on mordenite (Figure 2). These results were comparable with those obtained for Mn on the same zeolites. On ZSM-5, however, Cu showed stronger adsorption (~0.3 μmol m^{-2}) than shown by either Mn (~0.09 μmol m^{-2}) or Ca (~0.17 μmol m^{-2}) under the same conditions. Copper adsorption on ZSM-5 was still not as high as was observed on mordenite (~0.35 μmol m^{-2}). The adsorption of Cu on ZSM-5 was also not as great as the adsorption of Na in the presence of Ca (~0.60 μmol m^{-2}; Ferreira and Schulthess, 2011) on a molar basis, but the two results are comparable on an equivalents basis. Na adsorption on ZSM-5 was much less in the presence of Cu (~0.16 μmol m^{-2}) than in the presence of Mn (0.44 μmol m^{-2}) (data not shown). Furthermore, the adsorption of Na in the presence of Mn and the adsorption of Na in the presence of Ca are comparable, while the adsorption of Na in the presence of Cu is closer to that of Na in the presence of K (~0.15 μmol m^{-2}) (Ferreira and Schulthess, 2011), which was a strong competitor. This is consistent with the strong adsorption of Cu, which was comparable to the strongly adsorbing K, and weak adsorption of Mn, which was comparable to the weakly adsorbing Ca, on ZSM-5. Furthermore, this shows that the divalent ions are competing with Na for the same adsorption sites on the mineral surface.

https://doi.org/10.1346/CCMN.2012.0600604 Published online by Cambridge University Press

The hydrated diameter of Cu^{2+} (0.808 nm) and Mn^{2+} (0.878 nm) are comparable to that of Ca^{2+} (0.824 nm) but much larger than that of Na^{+} (0.730 nm) (Schulthess, 2005). The nanopore channel of zeolite Y is almost large enough to accommodate Mn and Cu in their hydrated state. In order to fit into the smaller nanopore channels of ZSM-5 and mordenite, however, they would be forced to shed part of their hydration spheres.

The NISE theory states that the unusual selectivity of monovalent ions over divalent cations in the medium nanopores is due to the fact that divalent ions have, in general, a much higher energy of hydration than monovalent ions (Hummer *et al.*, 1996). The greater an ion's energy of hydration, the more difficult it will be for that ion to dehydrate and adsorb inside nanopores where solvent density is decreased and dehydration is stabilized (Wang *et al.*, 2003). In the large nanopores of zeolite Y, ions can fit inside the nanopores without dehydrating and, therefore, the adsorption of both monovalent and divalent ions is weak. Mordenite's narrowest nanopores, however, are small enough that even a strongly hydrated ion must dehydrate in order to fit, and both monovalent ions and divalent ions adsorb equally strongly. Mordenite's large nanopores should behave similarly to those of zeolite Y. Previous Na-NMR research on mordenite showed that 87% of Na adsorbed in the small nanopores compared to 13% in the large pores based on chemical shift calculations (Ferreira *et al.*, 2012). The medium nanopores of ZSM-5 are small enough to stabilize dehydration, but large enough that a strongly hydrated ion could remain hydrated and adsorb instead *via* an outer-sphere mechanism.

Clearly, Cu is adsorbing more strongly than the other divalent ions studied in the medium nanopores of ZSM-5. An explanation for this inconsistency is that Cu is subject to the Jahn-Teller effect, which causes a tetragonal distortion in the coordination of its hydration sphere. As a result of the Jahn-Teller-induced distortion, Cu ions have two water molecules in their primary hydration spheres that are weakly bonded. Although Cu ions have a high total hydration energy for all six water molecules (Burgess, 1978), the weakness caused by the Jahn-Teller effect makes them susceptible to the loss of two of their hydrating water molecules in contrast to the very strong bonds that retain the other four water molecules (Cotton and Wilkinson, 1988, p. 770). In the nanopores where solvent density is decreased (Wang *et al.*, 2003), this weak bond in the hydration sphere caused by the Jahn-Teller effect would be particularly fragile. Loss of even one water molecule would allow the Cu ion to adsorb more closely to the mineral surface than other divalent ions and, in turn, explain the unusually strong adsorption of Cu on ZSM-5. Direct spectroscopic investigation of the behavior of divalent ions in the different sized nanopores is presented below to verify the predictions of the NISE theory regarding the adsorption mechanisms of divalent ions in these nanopore channels.

EPR spectroscopy

Competition with protons can affect the ability of cations to adsorb. This competition is reflected in the location of the adsorption edge of a competing cation. At pH values above the adsorption edge, competition with protons is weak compared to competition at pH values below the adsorption edge. Accordingly, the samples prepared for EPR analysis were analyzed at pH values above the adsorption edge.

Electron paramagnetic resonance experiments were conducted at ~pH 5.3 for Mn and ~pH 2.5 for Cu. These pH values were selected to optimize adsorption density while avoiding precipitation conditions. Any EPR spectrum asymmetry and peak broadening are evidence of anisotropy in the electron cloud or an interaction that hinders the ability of an ion's electrons to tumble freely in space (Carl and Larsen, 2000). An EPR spectrum shows asymmetry and peak broadening when the ion is in an environment where interactions (such as with a mineral surface or another ion) exist that hinder the ability of the electrons to tumble. Conversely, sharp narrow symmetrical peaks are observed when the ion's electrons are perfectly free to tumble because the vast majority of measurements will be close to the average value. Turkevich *et al.* (1972) showed that the EPR spectra of Cu adsorbed on zeolite Y increased in asymmetry as a function of dehydration due to a decrease in Cu mobility. Hronsky *et al.* (1978) showed that increased adsorption of Mn ions onto silica gel caused a corresponding increase in spectrum asymmetry after the specimen had been dried at 50ºC. They attributed this spectrum asymmetry to a disruption of the isotropy of the electron distribution around the Mn ion. When the Mn ion is fully hydrated, the distribution of the electrons is isotropic as the electrons are shared equally with the coordinated H_2O molecules around the ion. When one of these bonds is replaced by a bond with a surface oxygen, the electron distribution becomes less isotropic, resulting in a corresponding asymmetry in the EPR spectrum.

For the objectives of the present study, in which no drying of the specimens was performed, the symmetry of the adsorbed ion's electron cloud is the only EPR parameter necessary to determine if it is adsorbed *via* an inner-sphere or outer-sphere mechanism. Asymmetry in EPR spectra may be due to interaction with a surface, but can also be due to interaction with a neighboring ion (known as spin-spin interaction). Either interaction can cause a disruption in the isotropy of the ion's electron configuration. As spin-spin interactions require that the ions be close to each other, spin-spin interactions are unlikely to be present if the adsorbed ions are far from each other.

Based on the number of adsorbed ions per unit cell present in the sample, a three-dimensional model of each zeolite was used to calculate the distance between

https://doi.org/10.1346/CCMN.2012.0600604 Published online by Cambridge University Press

adsorbed ions. Details of these calculations are presented in the materials and methods section. On zeolite Y, the average distance between adsorbed Cu ions was determined to be 2.4 nm and the distance between adsorbed Mn ions was determined to be 3.2 nm. On ZSM-5, the average distance between adsorbed Mn ions was determined to be 2.86 nm and the distance between adsorbed Cu ions was determined to be 2.0 nm. On mordenite, the nearest distance between adsorbed Mn ions was determined to be 1.96 nm, and the nearest distance between adsorbed Cu ions was determined to be 1.81 nm.

Peak broadening due to spin-spin interaction occurs as a function of the cube of the distance between the atoms (Rabenstein and Shin, 1995). At a distance of 2.5 nm (the maximum distance for which the Rabenstein and Shin (1995) calculations have been verified), the broadening caused by spin-spin interactions is at most 0.00145 G, which is negligible considering the size of the peaks observed. The Rabenstein-Shin calculations show that spin-spin interaction at a separation distance of 1.0 nm is only 0.023 G, which is still very small when compared with the extent of the peak broadening observed on the spectra discussed below (~500 G, which corresponds to a *g* value of ~0.3). Accordingly, a spin-spin interaction occurring between the adsorbed Mn or Cu ions on any of the zeolites studied seems unlikely. Any asymmetry observed for the adsorbed ions on mordenite must, therefore, be due to a close interaction with the mineral surface (*i.e.* inner-sphere adsorption). This is logical because the zeolites used in this study had high SiO_2/Al_2O_3 ratios resulting in a physical separation of adsorption sites and, consequently, a physical separation of the adsorbed ions. As the adsorbed ions were located in distinct, independent locations, no strong interactions should have occurred between them, especially when compared to the interaction between an inner-sphere adsorbed ion and the mineral surface immediately adjacent to it. Furthermore, peak broadening caused by spin-spin interactions is generally symmetrical, which is not the case for the peak broadening observed for Mn adsorbed on mordenite (Figure 3). Similarly, the peak broadening observed for Cu adsorbed on ZSM-5 and mordenite (Figure 4) is probably due to an interaction with the surface and not to spin-spin interactions between adsorbed Cu ions.

The spectrum for Mn adsorbed on zeolite Y (Figure 3) is very similar to the spectrum for aqueous Mn in the supernatant shown at the top of the figure. The adsorbed Mn spectrum shows very little asymmetry. Some slight peak broadening was visible when compared to the aqueous spectrum (*i.e.* the zeolite Y spectrum begins to separate from the baseline at a *g* value of ~2.5, while the aqueous spectrum does not begin to rise above the baseline until a *g* value of 2.2). This indicates some interaction between the Mn ion and the mineral surface,

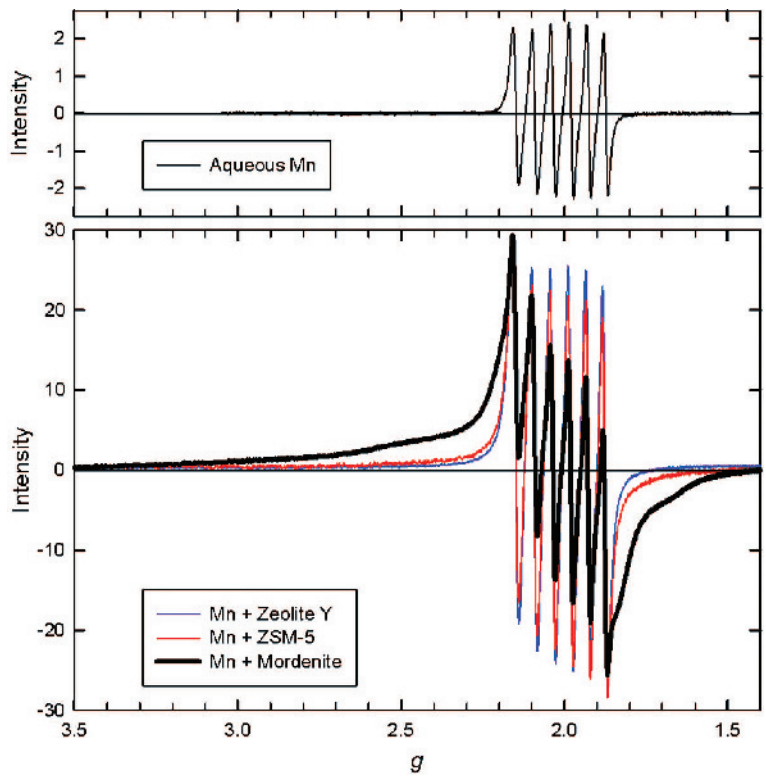

Figure 3. Normalized EPR spectra of adsorbed Mn at pH 5.3 on zeolite Y, ZSM-5, and mordenite.

https://doi.org/10.1346/CCMN.2012.0600604 Published online by Cambridge University Press

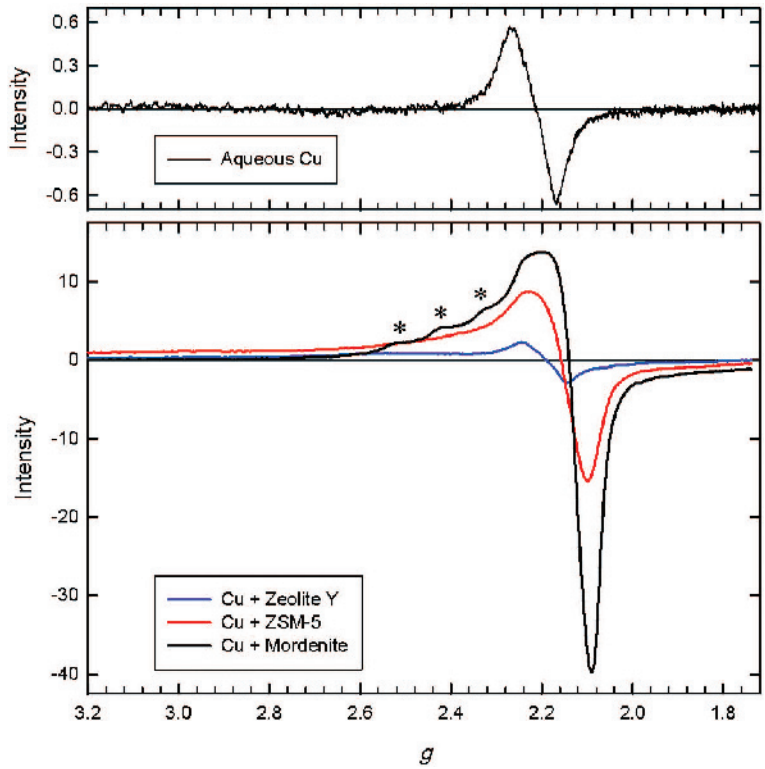

Figure 4. EPR spectra of adsorbed Cu at pH 2.5 on zeolite Y, ZSM-5, and mordenite. Hyperfine features for Cu adsorbed on mordenite are indicated with asterisks (*).

but it is very subtle. The Mn ion is, therefore, predominantly adsorbing *via* an outer-sphere mechanism.

The spectrum for Mn adsorbed on ZSM-5 (Figure 3) is similar to that of Mn adsorbed on zeolite Y. A similar slight asymmetry and peak broadening was visible in the shape of the spectrum when compared to the supernatant Mn. As the solid-phase spectrum is mostly symmetrical and overlays so closely with the supernatant spectrum, one can reasonably describe the Mn ions as remaining mostly hydrated and adsorbing *via* an outer-sphere mechanism on ZSM-5 also.

The spectrum for adsorbed Mn on mordenite (Figure 3), however, is both extremely broad and highly asymmetrical. The peak broadening starts at a much lower field (*g* value of 3.3) and ends at a much higher field (*g* value of 1.5) on mordenite than it did for either ZSM-5 or zeolite Y. The asymmetry is also stronger on mordenite. This indicates that the level of interaction with the mordenite surface is quite strong, and certainly stronger than on ZSM-5 or zeolite Y. The adsorption of Mn on mordenite at pH 5.3 is 0.275 μmol m^{-2}, equivalent to 0.550 μmol_c m^{-2} as Mn is primarily in the form of the Mn^{2+} ion at this pH. Sodium retention at this pH in the presence of Mn was 0.10 μmol m^{-2} (data not shown). Thus, the site density is ~0.65 μmol_c m^{-2}, which agrees with the 0.60 μmol m^{-2} adsorption capacity of mordenite at pH 5.3 based on Na retention reported by Ferreira and Schulthess (2010). Accordingly, at pH 5.3, the cation exchange complex is 85% saturated with Mn and the adsorption sites are located primarily in the small channels (Alberti *et al.*, 1986; Simoncic and Armbruster, 2004). The EPR spectrum (Figure 3) suggests, therefore, that a substantial fraction of the Mn ions on mordenite is adsorbing *via* an inner-sphere mechanism, and this agrees with the strong adsorption data (Figure 1).

A series of EPR spectra were also obtained for Cu on the three zeolites (Figure 4). The spectrum for the aqueous Cu in the supernatant is displayed at the top of the figure. The EPR spectrum for Cu adsorbed on zeolite Y is very symmetrical, although some peak broadening is present. The Cu ions adsorbed on zeolite Y experience an environment very similar to that experienced by aqueous Cu ions in the supernatant, indicating that the Cu on zeolite Y is fully hydrated and must, therefore, be adsorbing *via* an outer-sphere mechanism.

The spectrum for Cu adsorbed on ZSM-5 (Figure 4) shows significant asymmetry compared to the supernatant spectrum. The negative lobe of the spectrum is larger than the positive lobe of the spectrum, and the entire spectrum is also shifted to lower *g* values. Peak broadening of the solid-phase spectrum is also clearly visible. Both the peak broadening and the spectrum asymmetry are indications of a strong interaction between the adsorbed Cu ion and the mineral surface of ZSM-5. The adsorption of Cu on ZSM-5 at pH 2.5 is

https://doi.org/10.1346/CCMN.2012.0600604 Published online by Cambridge University Press

0.27 μmol m^{-2}, equivalent to 0.54 μmol_c m^{-2} as Cu is primarily in the form of the Cu^{2+} ion at this pH. Sodium retention at this pH in the presence of Cu was 0.08 μmol m^{-2} (data not shown). The site density is ~0.78 μmol_c m^{-2} (Ferreira and Schulthess, 2010), which includes H^+, Na^+, and Cu^{2+}. Accordingly, the EPR spectrum of Cu on ZSM-5 corresponds to a cation exchange complex that is 70% saturated with Cu. Given that the ZSM-5 nanopore channels are all nearly identical, this EPR evidence of strong surface interaction (Figure 4) indicates that a substantial fraction of the Cu is adsorbed *via* an inner-sphere mechanism.

The adsorption of Cu on mordenite at pH 2.5 is 0.346 μmol m^{-2}, equivalent to 0.692 μmol_c m^{-2} as Cu is primarily in the form of the Cu^{2+} ion at this pH. Sodium retention at this pH in the presence of Cu was <0.05 μmol m^{-2} (data not shown). Thus, the site density is <0.74 μmol_c m^{-2}, which is comparable to the site density estimate made earlier with Mn. Accordingly, the EPR spectrum of Cu on mordenite (Figure 4) corresponds to a cation exchange complex that is at least 94% saturated with Cu.

The spectrum for Cu adsorbed on mordenite (Figure 4) is similar to that of the Cu adsorbed on ZSM-5, but with the asymmetry even more pronounced. Some hyperfine features are also present from *g* values of 2.6 to 2.3 in the spectrum for Cu adsorbed on mordenite that are not present in the spectrum for Cu adsorbed on ZSM-5. Larsen *et al.* (1994) observed that hyperfine features appeared in the EPR spectra for samples of Cu adsorbed on ZSM-5 at 77 K at room humidity and for samples heated to 723 K under vacuum and then analyzed at room temperature. The features were not visible, however, on a sample analyzed at 298 K at room humidity. The authors reasoned that these peaks are indicative of Cu dehydration and a high degree of immobility. Accordingly, the presence of these features in Figure 4 indicates that a substantial fraction of the Cu adsorbed on mordenite is also adsorbed *via* an inner-sphere mechanism, but it is bound more tightly to the mineral surface on mordenite than it is on ZSM-5. This is reasonable because the mordenite channels are smaller and more able to constrain the mobility of Cu ions held inside them. The evidence for inner-sphere Cu adsorption on ZSM-5 and mordenite agrees with the adsorption data (Figure 2) that showed strong Cu retention on these two zeolites.

In addition to spectral broadening and the development of asymmetry, some readily quantifiable parameters can be derived from the EPR spectra (Table 3). The effective *g* factor (*g*), which indicates the degree of interaction of the electron with local spins arising from other electrons or magnetic nuclei in the immediate environment, is often a sensitive probe of bonding mechanisms. Generally, *g* is compared to the value obtained for the 'free' electron, g_e, which is a physical constant equal to 2.002319. The ratio of g/g_e quantifies the degree to which the electronic environment of the unpaired electron(s) differs from that of the free electron. Also, removal of orbital degeneracy due to interactions of the orbitals with magnetic nuclei (nuclear spins of ^{55}Mn = 5/2 and of ^{63}Cu and ^{65}Cu = 3/2) leads to a hyperfine spectrum superimposed over the main absorption spectrum. The spacing of peaks in the hyperfine spectrum is quantified by the hyperfine splitting constant, A, and has been suggested to be sensitive to the displacement of waters of hydration by other ligands such as OH or oxygen anions associated with the zeolite surface (Doula and Dimirkou, 2008).

As shown in Table 3, the effective value of *g* obtained for the aqueous Mn ion is very similar to that for the free electron (g/g_e = 1.0030). Upon adsorption, the value increases slightly to 1.0039, and with inner-sphere adsorption (mordenite) retreats slightly to 1.0038. The slight increase in *g* reflects the perturbation of the electronic environment as a result of adsorption to a state that is more restricted than that of the aqueous ion. The value for *A* is essentially unchanged for all four Mn spectra. However, aside from indicating that the ion is adsorbed, the *g* and *A* parameters derived from Mn EPR spectra seem relatively insensitive to the adsorption mechanism, probably because of the extra stability afforded by the d^5 electronic configuration and the lack of coupling between electronic orbitals.

Table 3. EPR spectral parameters. Some A values could not be calculated (noted as n/a) because they lacked hyperfine features. Relative shift = $(g-g_e)/(g_{aq}-g_e)$.

Sample ID	Average *g*	g/g_e	Relative *g* shift	*A* (MHz)
Mn, aqueous	2.00835	1.0030	1.00	269
Mn, zeolite Y	2.01010	1.0039	1.29	269
Mn, ZSM-5	2.01014	1.0039	1.30	269
Mn, mordenite	2.00983	1.0038	1.25	269
Cu, aqueous	2.21253	1.1050	1.00	n/a
Cu, zeolite Y	2.18843	1.0929	0.89	n/a
Cu, ZSM-5	2.15722	1.0774	0.74	n/a
Cu, mordenite	2.14000	1.0688	0.65	404

https://doi.org/10.1346/CCMN.2012.0600604 Published online by Cambridge University Press

A much more sensitive EPR parameter response is seen for Cu. First, the unpaired electron in the aqueous Cu ion is substantially different from the free electron, yielding a g/g_e value of 1.1050 (Table 3). This value decreases with adsorption, and the trend to lower values continues as adsorption progresses from outer-sphere to inner-sphere. A similar trend was noted by Doula and Dimirkou (2008) and attributed to displacement of waters of hydration by surface ligands. The high sensitivity of the Cu EPR spectra to the adsorption mechanism probably stems from its innate instability as a result of the Jahn-Teller distortion, and suggests that as Cu adsorbs and the environment becomes more stable, this distortion decreases somewhat. A value for A is obtained only for the mordenite sample, where the highest degree of inner-sphere adsorption occurs, and where the most rigid coordination environment would be expected.

The adsorption data for Mn and Cu (Figures 1, 2) and the EPR spectroscopy data (Figures 3, 4) complement each other well. The adsorption envelopes showed weak Mn retention on zeolite Y and ZSM-5 and strong Mn retention on mordenite. This concurs with the EPR data that showed outer-sphere adsorption for Mn on zeolite Y and ZSM-5, and substantial inner-sphere adsorption on mordenite. Adsorption envelopes for Cu showed weak retention on zeolite Y and strong retention on ZSM-5 and mordenite. This agrees with the EPR spectra that showed Cu adsorbed *via* an outer-sphere mechanism on zeolite Y, and increasingly *via* an inner-sphere mechanism on ZSM-5 and mordenite.

CONCLUSIONS

The adsorption pattern for Mn agrees with the predictions made by the NISE theory for divalent cations based on the adsorption envelopes generated for Na, K, and Ca (Ferreira and Schulthess, 2011). The fact that a substantial fraction of the Cu adsorbed via an inner-sphere mechanism on ZSM-5, however, indicates that the predictions of the NISE theory should consider step-wise hydration energies to describe an ion's dehydration potential. This is evident, for example, with an ion such as Cu, which is subject to the Jahn-Teller effect and where hydration energies of two of the coordinating waters are considerably smaller than would be expected from normal octahedral coordination.

Evidence in support of the NISE theory has been collected by adsorption envelopes (Schulthess *et al.*, 2011; Ferreira and Schulthess, 2011), NMR spectroscopy (Ferreira *et al.*, 2012), flow calorimetry (Ferreira *et al.*, 2013), and EPR spectroscopy (this study). Divalent cations are generally considered to be strongly retained by mineral surfaces, particularly under dry conditions (Larsen *et al.*, 1994; Carl and Larsen, 2000). This EPR study, however, presented evidence that they can adsorb weakly *via* an outer-sphere mechanism in moist environments. The behavior of these ions in constrained environments may be important when considering their retention and transport in soil and groundwater.

ACKNOWLEDGMENTS

The present study was supported financially by the project 'Ion exchange processes in nanopores, clay interlayers and sodic soils' (USDA-Hatch no. CONS00864), funded by the United States Department of Agriculture.

The EPR spectra were collected at EMSL, a national scientific user facility sponsored by the U.S. Department of Energy's (DOE) Office of Biological and Environmental Research and located at Pacific Northwest National Laboratory (PNNL). The PNNL is operated by Battelle for DOE under contract DE-AC05-76RL01830.

REFERENCES

Alberti, A., Davoli, P., and Vezzalini, G. (1986) The crystal structure refinement of a natural mordenite. *Zeitschrift für Kristallographie*, **175**, 249–256.

Bergaoui, L., Lambert, J.-F., Suquet, H., and Che, M. (1995) Cu^{II} on Al_{13}-pillared saponites: Macroscopic adsorption measurements and EPR spectra. *Journal of Physical Chemistry*, **99**, 2155–2161.

Burgess, J. (1978) *Metal Ions in Solution*. Ellis Horwood Limited, Sussex, England.

Carl, P.J. and Larsen, S.C. (2000) EPR study of copper-exchanged zeolites: Effects of correlated g- and A-strain, Si/Al ratio, and parent zeolite. *Journal of Physical Chemistry*, **104**, 6568–6575.

Collins, K.D. (1997) Charge density-dependent strength of hydration and biological structure. *Biophysical Journal*, **72**, 65–76.

Cotton, F.A. and Wilkinson, G. (1988) *Advanced Inorganic Chemistry*, 5th edition. John Wiley & Sons, New York.

Doula, M.K. and Dimirkou, A. (2008) An EPR study of Cu adsorption by clinoptilolite from Cl^-, NO_3^- and SO_4^{2-} solutions. *Journal of Porous Materials*, **15**, 457–466.

Ferreira, D.R. (2012) The nanopore inner-sphere enhancement (NISE) effect and its role in sodium retention. PhD Dissertation, University of Connecticut, USA, 181 pp., AAT 3529380.

Ferreira, D.R. and Schulthess, C.P. (2011) The nanopore inner sphere enhancement effect on cation adsorption: Sodium, potassium, and calcium. *Soil Science Society of America Journal*, **75**, 389–396.

Ferreira, D.R., Schulthess, C.P., and Giotto, M.V. (2012) An investigation of strong sodium retention mechanisms in nanopore environments using nuclear magnetic resonance spectroscopy. *Environmental Science & Technology*, **46**, 300–306.

Ferreira, D.R., Schulthess, C.P., and Kabengi, N.J. (2013) Calorimetric evidence in support of the nanopore inner-sphere enhancement (NISE) theory on cation adsorption. *Soil Science Society of America Journal.* DOI 10.2136/sssaj2012.0140.

Hronský, V., Rákoš, M., Belák, J., and Kazár, D. (1978) EPR study of Mn^{2+} ions adsorption on silica gel. *Czechoslovak Journal of Physics B*, **28**, 1277–1286.

Hummer, G., Pratt, L.R., and García, A.E. (1996) Free energy of ionic hydration. *Journal of Physical Chemistry*, **100**, 1206–1215.

Larsen, S.C., Aylor, A., Bell, A.T., and Reimer, J.A. (1994)

Electron paramagnetic resonance studies of copper ion-exchanged ZSM-5. *Journal of Physical Chemistry*, **98**, 11533–11540.

Rabenstein, M.D. and Shin, Y.-K. (1995) Determination of the distance between two spin labels attached to a macromolecule. *Proceedings of the National Academy of Sciences USA*, **92**, 8239–8243.

Schulthess, C.P. (2005) *Soil Chemistry with Applied Mathematics*. Trafford Publishers, Victoria, BC, Canada.

Schulthess, C.P., Taylor, R.W., and Ferreira, D.R. (2011) The nanopore inner sphere enhancement effect on cation adsorption: Sodium and nickel. *Soil Science Society of America Journal*, **75**, 378–388.

Simoncic, P. and Armbruster, T. (2004) Peculiarity and defect structure of the natural and synthetic zeolite mordenite: A single-crystal X-ray study. *American Mineralogist*, **89**, 421–431.

Sposito, G. (1989) Surface reactions in natural aqueous colloidal systems. *Chimia*, **43**, 169–176.

Turkevich, J., Ono, Y., and Soria, J. (1972) Futher electron spin resonance studies of Cu(II) in Linde Y zeolite. *Journal of Catalysis*, **25**, 44–54.

Wang, Y., Bryan, C., and Xu, H. (2003) Nanogeochemistry: Geochemical reactions and mass transfer in nanopores. *Geology*, **31**, 387–390.

(*Received 8 August 2012; revised 23 November 2012; Ms. 698; AE: S. Kuznicki*)